Hindawi Publishing Corporation
EURASIP Journal on Applied Signal Processing
Volume 2006, Article ID 82023, Pages 1–12
DOI 10.1155/ASP/2006/82023

Joint Source-Channel Coding by Means of an Oversampled Filter Bank Code

Slavica Marinkovic and Christine Guillemot

IRISA-INRIA, Campus de Beaulieu, 35042 Rennes Cedex, France

Received 1 September 2004; Revised 5 April 2005; Accepted 7 April 2005

Quantized frame expansions based on block transforms and oversampled filter banks (OFBs) have been considered recently as joint source-channel codes (JSCCs) for erasure and error-resilient signal transmission over noisy channels. In this paper, we consider a coding chain involving an OFB-based signal decomposition followed by scalar quantization and a variable-length code (VLC) or a fixed-length code (FLC). This paper first examines the problem of channel error localization and correction in quantized OFB signal expansions. The error localization problem is treated as an M-ary hypothesis testing problem. The likelihood values are derived from the joint pdf of the syndrome vectors under various hypotheses of impulse noise positions, and in a number of consecutive windows of the received samples. The error amplitudes are then estimated by solving the syndrome equations in the least-square sense. The message signal is reconstructed from the corrected received signal by a pseudoinverse receiver. We then improve the error localization procedure by introducing a per-symbol reliability information in the hypothesis testing procedure of the OFB syndrome decoder. The per-symbol reliability information is produced by the soft-input soft-output (SISO) VLC/FLC decoders. This leads to the design of an iterative algorithm for joint decoding of an FLC and an OFB code. The performance of the algorithms developed is evaluated in a wavelet-based image coding system.

1. INTRODUCTION

Various joint source-channel coding approaches, guided by an optimum tradeoff between compression efficiency and error and/or erasure resilience depending on the link characteristics, have been considered in order to improve multimedia signal transmission over noisy channels. Here, we focus on JSCC techniques based on quantized redundant signal expansions by means of OFB. As the signal representation in this approach is redundant, an OFB-encoded stream has error-resilient features. Error-control coding and signal decomposition are thus integrated in a single block. The error-correcting code thus allows also to suppress some quantization noise effects.

So far, the research in this area has been concentrated mainly on the study of oversampled transform codes (OTC) which are OFB codes with polyphase filter orders equal to zero. The OTC can be viewed as real-number block codes, while the OFB codes can be associated to real-number convolutional codes. Decoding of real-number block codes has been considered by many authors [1–7]. Oversampled block transforms like DFT codes have been shown to be BCH codes over the real field [8, 9]. DFT or DCT codes have also been considered as joint source-channel block codes to obtain robustness to erasures [4–6, 10] and impulse noise errors [2, 3, 11–13]. Filter bank frame expansions have also been studied to achieve resilience to erasures [14–16]. In [14], the authors have shown correspondences between OFB and frames in $l^2(Z)$. They have shown that if the frames satisfy some properties, the mean-square reconstruction error can be minimized. The authors in [17] have studied oversampled tree-structured filter banks for erasure recovery. However, there has not been many studies of OFB codes for impulse error correction.

Here we consider OFB-based quantized redundant signal expansions for both signal compression and channel error recovery. The problem of decoding OFB codes can be viewed as a problem of decoding real-number convolutional codes in presence of impulse noise errors and background noise [18, 19]. In contrast to finite-field convolutional codes, real-numbered convolutional codes have infinite state-space size, and therefore Viterbi algorithm cannot be applied. The decoding strategy which is usually considered is based on syndrome decoding [8, 18]. This problem has been treated in [18] in the context of fault-tolerant systems and channel coding for communications, and recently in [19] in the context of JSCC. Presence of background noise requires different error localizations and calculation procedures to be

used than that of standard syndrome decoding. The localization procedure usually relies on the hypothesis testing theory. For example, in both [18, 19], the error localization is motivated by the M-ary hypothesis testing theory. However, they differ in the way the likelihood values for hypothesis testing are calculated. In [18], the activity detection (presence of impulse errors) is based on forming the quadratic terms for each log-likelihood ratio calculated from the syndrome covariance matrices under various hypotheses. In [19], the error localization is based on the pdf of syndrome norm.

The error localization procedure presented here is inspired from [18]. However, in contrast to [18] where the detection of the increased noise statistics due to impulse errors employs quadratic forms of likelihood ratios [1, 18], we apply a minimum total probability of error test [20]. That is, we compute the a posteriori probability of each hypothesis, and choose the largest. We consider two channel impulse noise models. We first consider a Bernoulli-Gaussian impulse noise model as in [18, 19]. We then introduce a quantizer-dependent impulse noise model. This model takes into account the discrete nature of the impulse errors at the output of the VLC/FCL decoders. For these two impulse noise models, the error localization procedure based on M-ary hypothesis testing theory is presented. Each possible error position within a window of the received samples is considered as a separate hypothesis. The localization procedure selects the hypothesis with a maximum a posteriori probability. The error amplitudes are then estimated by solving the syndrome equations in the least-square sense. The message is reconstructed from the corrected received sequence by a pseudoinverse receiver. We further consider using the soft information, that is, per-symbol reliability information, produced by the SISO VLC/FLC decoder in the localization procedure of the OFB decoder. The a posteriori probabilities of the source symbols produced by the SISO VLC/FCL decoders are used in the calculation of the hypothesis a priori probabilities. The results show that introducing the soft information in the error localization procedure in this way improves the probability of detection and decreases the MSE. An iterative algorithm for joint decoding of the FLC and an OFB code is presented. In this algorithm, the trellis for the decoding of the FLC-encoded source coefficients modeled by the first-order Markov source is iteratively pruned with the help of the hypothesis a posteriori probabilities. This is done based on the information on the symbols for which errors have been detected in the OFB syndrome decoder. The performance of these algorithms has been tested in the image compression system based on the subband decomposition by a wavelet filter bank.

The paper is organized as follows. Section 2 introduces the general framework and problem statement. OFB codes are described in Section 3. Section 4 describes the SISO VLC/FLC decoders. The impulse error models and the OFB syndrome decoding algorithms are described in Section 5. Iterative algorithm for decoding of the FLC and OFB chain is presented in Section 6. Simulation results are given in Section 7.

2. GENERAL FRAMEWORK AND PROBLEM STATEMENT

The block diagram of the considered encoding/decoding chain is shown in Figure 1. The encoding chain consists of an OFB followed by a scalar quantization and a fixed or variable-length coder. An OFB provides an oversampled frame expansion of the input signal. A set of vectors $\Phi = \{\phi_i\}_{i\in\mathbb{I}}$ in a Hilbert space $\mathbb{H}$ is a frame if for any $\mathbf{x} \neq 0$,

$$A\|\mathbf{x}\|^2 \leq \sum_{i\in\mathbb{I}} |\langle \mathbf{x}, \phi_i\rangle|^2 \leq B\|\mathbf{x}\|^2, \tag{1}$$

where $\langle \mathbf{x}, \mathbf{y}\rangle$ denotes the inner product of $\mathbf{x}$ and $\mathbf{y}$, $\mathbb{I}$ is the index set, and $A > 0$, and $B < \infty$ are constants called frame bounds [14]. The coefficients of the expansion are quantized and encoded. In the sequel, both fixed- and variable-length codes are considered. When considering a system with a variable-length code (VLC), we employ a scalar quantizer with a dead zone and with a number of levels N_Q^k for each subband k, $k = 0, \ldots, N-1$. In the system with an FLC, we employ a Lloyd-Max scalar quantizer with the same number of quantization levels N_Q^k. The encoded subbands are transmitted over an additive white Gaussian noise (AWGN) channel. Overcomplete frame expansions for providing robustness to erasures and errors in communication networks can be regarded as joint source-channel codes. The redundancy inherent in a frame makes the expansion resilient to additive channel and quantization noise. Similarly, the implicit redundancy due to the use of FLC or due to VLC coder suboptimality in capturing the Markov property of the OFB outputs gives extra error-correcting capability. The receiver consists of a SISO VLC/FLC decoder followed by the inverse quantization, OFB syndrome decoder, and a synthesis filter bank.

In Figure 1, the message signal is denoted by $x[n]$. A sample at time instant n of the signal in subband k at the output of the OFB is denoted by $y^k[n]$. In the sequel, L^k denotes the number of samples (or symbols) in subband k. Each quantized coefficient $y_q^k[n]$ in subband k takes its value in an alphabet of dimension N_Q^k. The sequence of quantized symbols in subband k is denoted by $y_q^k[n]$. The vector $\mathbf{u}^k[n] = [u_0^k[n] \cdots u_{l_c^k[n]-1}^k[n]]$ denotes the VLC/FLC codeword corresponding to symbol $y_q^k[n]$, where $l_c^k[n]$ is the length of the VLC/FLC codeword. In the case of FLC, $l_c^k[n] = l_c^k$. The BPSK modulated VLC/FLC codewords and the channel observations corresponding to these codewords in subband k are denoted by $\mathbf{c}^k[n] = [c_0^k[n] \cdots c_{l_c^k[n]-1}^k[n]]$ and $\mathbf{z}^k[n] = [z_0^k[n] \cdots z_{l_c^k[n]-1}^k[n]]$, respectively. The estimates of the received symbols at the output of the VLC/FLC decoder in subband k are denoted by $y_R^k[n]$. The symbol a posteriori probabilities calculated by VLC/FLC decoders in subband k are denoted by $P^k[n]$. The estimate of the kth subband signal at the output of the OFB syndrome decoder is denoted by $\hat{y}^k[n]$ and the estimate of the message signal is denoted by $\hat{x}[n]$.

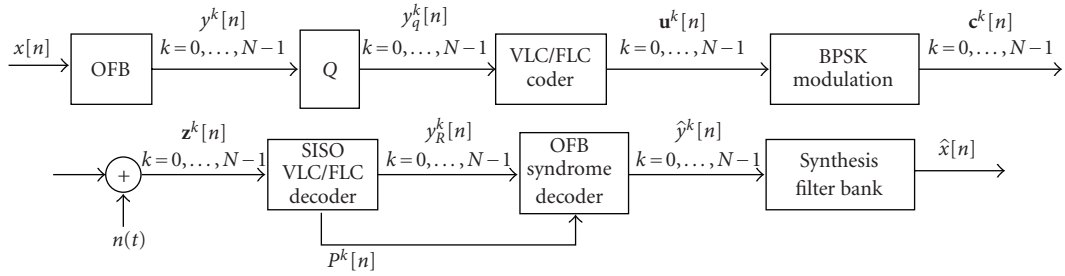

Figure 1: Joint source-channel coding chain considered.

3. OVERSAMPLED FILTER BANK CODES

There are numerous ways to construct oversampled filter banks [15, 21–23]. A straightforward approach that often yields an OFB from critically uniform FBs is by replacing the downsampling factor to a number less than the number of channels.

The OFB codes constructed in this way may not have the best error-correction power, however they can be very simply integrated in current source-coding standards.

Let us consider the analysis and synthesis filter banks with N filters shown in Figure 2. In the analysis filter bank, an input signal $x[n]$ is split into N signals $y^k[n]$, $k = 0, \ldots, N-1$. The sequence $y^k[n]$ is obtained by downsampling the output of the filter k with a factor K, where $K \leq N$. The sequences $y^k[n]$ are then quantized and transmitted over the channel. The task of the receiver is to combine the received signals into a single signal $\hat{x}[n]$ which, in absence of quantization, is identical to the signal $x[n]$, and which, in presence of quantization, is as close as possible to $x[n]$ in the mean-square error sense. Due to redundant signal representation ($K < N$), perfect reconstruction (PR) may be possible even if some of the signals $y^k[n]$ are corrupted.

The encoding operation performed by an OFB with N channels and downsampling factors K can be described in the polyphase domain as

$$\mathbf{Y}(z) = \mathbf{E}(z)\mathbf{X}(z), \tag{2}$$

where $\mathbf{X}(z)$ and $\mathbf{Y}(z)$ are the polyphase representations of the input and the output signals for the analysis filter bank and $\mathbf{E}(z)$ is an $[N \times K]$ analysis polyphase matrix [24].As OFB implement processing analog to that implemented by convolutional codes, the analysis matrix $\mathbf{E}(z)$ is referred to as a generator matrix of an OFB code. Similarly, the parity check matrix is defined as

$$\begin{aligned} \mathbf{P}(z)\mathbf{E}(z) &= \mathbf{0}, \\ \mathbf{P}(z) &= \sum_{i=0}^{L_P} \mathbf{P}_{L_P - i} z^{-i}, \end{aligned} \tag{3}$$

where $\mathbf{P}_i$ is a $[(N-K) \times N]$ matrix and where L_P denotes the order of the multiple-input multiple-output parity check filter. From (2) and (3), we observe that filtering a sequence $\mathbf{Y}(z)$ with parity check filters yields zero sequences. On the other hand, if the transmitted signal is corrupted by quantization noise and errors, we have

$$\mathbf{S}(z) = \mathbf{P}(z)\big(\mathbf{Y}(z) + \mathbf{e}(z) + \mathbf{n}(z)\big) = \mathbf{P}(z)\big(\mathbf{e}(z) + \mathbf{n}(z)\big), \tag{4}$$

where $\mathbf{n}(z)$ is the quantization noise, and $\mathbf{e}(z)$ denotes error sequences in various subbands. $\mathbf{S}(z)$ denotes a vector of z transforms of the sequences at the parity check filters outputs. The parity check outputs $\mathbf{S}(z)$ are referred to as syndromes.

Let us denote $(N-K)$ parity check filter outputs for time instant n by a vector

$$\mathbf{s}[n] = \begin{bmatrix} s^0[n] & \cdots & s^{(N-K)}[n] \end{bmatrix}^T. \tag{5}$$

And let the vectors

$$\begin{aligned} \mathbf{e}[n] &= \begin{bmatrix} e^0[n] & \cdots & e^{N-1}[n] \end{bmatrix}^T, \\ \mathbf{n}[n] &= \begin{bmatrix} n^0[n] & \cdots & n^{N-1}[n] \end{bmatrix}^T \end{aligned} \tag{6}$$

denote errors and quantization noise at the inputs to the $[(N-K) \times N]$ parity check filter at time instant n, respectively.

In the time domain, the syndrome equations for L time instants can be written as

$$\mathbf{S} = \mathbf{P}(\mathbf{e} + \mathbf{n}), \tag{7}$$

where $\mathbf{S}$ is an $(N-K)L$ vector of syndrome values given by

$$\mathbf{S} = \begin{bmatrix} \mathbf{s}^T[0] & \cdots & \mathbf{s}^T[L-1] \end{bmatrix}^T, \tag{8}$$

$\mathbf{e}$ is an $[N(L+L_P)]$ error vector given by

$$\mathbf{e} = \begin{bmatrix} \mathbf{0} & \cdots & \mathbf{0} & \mathbf{e}^T[0] & \ldots & \mathbf{e}^T[L-1] \end{bmatrix}^T, \tag{9}$$

$\mathbf{n}$ is an $[N(L+L_P)]$ vector containing quantization noise

$$\mathbf{n} = \begin{bmatrix} \mathbf{0} & \cdots & \mathbf{0} & \mathbf{n}^T[0] & \cdots & \mathbf{n}^T[L-1] \end{bmatrix}^T, \tag{10}$$

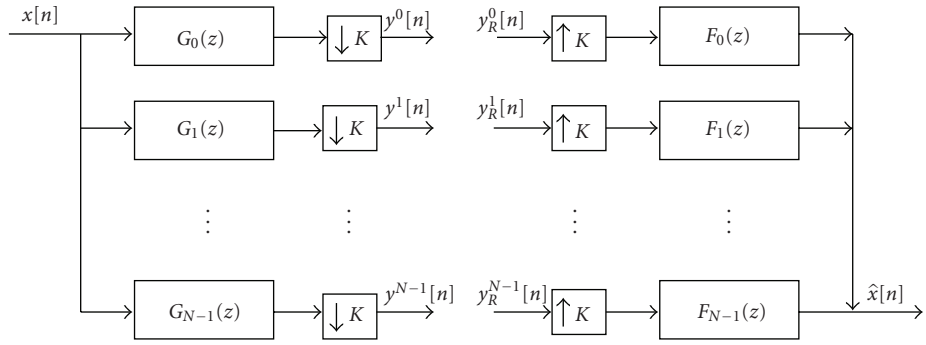

Figure 2: Oversampled filter bank structure.

and $\mathbf{P}$ is an $[(N-K)L \times N(L+L_P)]$ parity check matrix given by

$$\mathbf{P} = \begin{bmatrix} \mathbf{P}_0 & \mathbf{P}_1 & \cdots & \mathbf{P}_{L_P} & \mathbf{0} & \cdots & \cdots \\ \mathbf{0} & \mathbf{P}_0 & \mathbf{P}_1 & \cdots & \mathbf{P}_{L_P} & \mathbf{0} & \cdots \\ \vdots & \ddots & \ddots & \ddots & \ddots & \ddots & \ddots \\ \mathbf{0} & \cdots & \mathbf{0} & \mathbf{P}_0 & \mathbf{P}_1 & \cdots & \mathbf{P}_{L_P} \end{bmatrix}. \tag{11}$$

The matrix $\mathbf{P}_i$ is defined in (4). Note that first $L_P N$ elements of the error and quantization noise vectors are equal to zero. As in the case of codes over the finite field, the syndromes can be used to detect and correct errors.

4. SISO VLC/FLC DECODER

The performance of FLC and VLC decoding can be significantly improved by exploiting the correlation between the coefficients in a subband. The quantized coefficients in the subband k, $\mathbf{y}_q^k$, are modeled as a first-order Markov process with symbol alphabet $\mathcal{S}^k = \{S_0^k \cdots S_{N_Q^k-1}^k\}$. In this model, the sequence at the output of each subband is described by a vector of symbols' stationary probabilities $\mathbf{P}_{\text{st}}^k = [P(S_0^k) \cdots P(S_{N_Q^k-1}^k)]$ and the probability transition matrix $\mathbf{P}_t^k$ with entries $P_t^k(m,v) = P(S_v^k \mid S_m^k)$, $n, m = 0, \ldots, N_Q^k - 1$.

The SISO decoder uses a symbol-by-symbol maximum a posteriori probability criterion (also referred to as maximum posterior marginals—MPM) for estimating a sequence of subband coefficients. However, it also outputs per-symbol reliability information. That is, the decoder outputs a pair $(\hat{y}_q^k[n], P^k[n])$, where

$$\begin{aligned} \hat{y}_q^k[n] &= \arg\max_k P\left(y_q^k[n] = s \mid \mathbf{z}^k\right), \\ P^k[n] &= \max_k P\left(y_q^k[n] = s \mid \mathbf{z}^k\right), \quad s \in \mathcal{S}^k, \end{aligned} \tag{12}$$

and where $\mathbf{z}^k$ is a vector of all the observations at the input of the VLC/FLC decoder for subband k.

The derivation of the SISO decoding algorithm for FLC is straightforward. The channel observations corresponding to each symbol are gathered together. Symbol-by-symbol MAP estimation is done on the trellis defined by the Markov model for the subband coefficients [25].

The a posteriori probabilities of symbols in the SISO FLC decoders, for each subband k, are computed with the BCJR algorithm [26] in the following way:

$$\begin{aligned} P\left(y_q^k[n] \mid \mathbf{z}^k\right) &\propto \alpha_n(s)\beta_n(s), \quad \alpha_n(s) = P\left(y_q^k[n] = s, \mathbf{z}_{1,n}^k\right), \\ \beta_n(s) &= P\left(\mathbf{z}_{n+1,L^k}^k \mid y_q^k[n] = s\right), \end{aligned} \tag{13}$$

$$\begin{aligned} \gamma_n(s',s) &= P\left(y_q^k[n] = s, \mathbf{z}_n^k \mid y_q^k[n-1] = s'\right) \\ &= P(s \mid s') \prod_{v=0}^{l_c^k-1} \left(z_v^k[n] \mid c_v^k[n]\right), \quad s, s' \in \mathcal{S}^k, \end{aligned} \tag{14}$$

where $\mathbf{z}_n^k = [z_0^k[n] \; z_2^k[n] \; \cdots \; z_{l_c^k-1}^k[n]]$ are the observations corresponding to the quantized symbol $y_q^k[n]$, $\mathbf{z}_{n,v}^k = [\mathbf{z}_n^k \; \mathbf{z}_{n+1}^k \; \cdots \; \mathbf{z}_v^k]$ is a vector of observations corresponding to $y_q^k[n] \cdots y_q^k[v]$, and $\mathcal{S}^k$ is the symbol alphabet for subband k. The forward and backward steps consist in calculating $\alpha_n(s) = \sum_{s'} \alpha_{n-1}(s')\gamma_n(s',s)$ and $\beta_n(s) = \sum_{s'} \beta_{n+1}(s')\gamma_{n+1}(s,s')$. The coefficients $\alpha_0(s)$ are initialized with the stationary probabilities of the source symbols, and the coefficients $\beta_{L^k}(s)$ are initialized with uniform probability distribution.

In the case of a VLC, due to the variable-length property of the codewords, the estimation of the transmitted bit stream must be performed together with its segmentation [25]. That is, it is necessary to calculate the probability of the pair $P(y_q^k[n] = s, N_n^k = l \mid \mathbf{z}^k)$, where N_n^k is the number of bits in the VLC coding of the sequence $y_q^k[0], \ldots, y_q^k[n]$.The decoder outputs

$$\begin{aligned} \hat{y}_q^k[n] &= \arg\max_s \sum_l P\left(y_q^k[n] = s, N_n^k = l \mid \mathbf{z}^k\right), \\ \hat{P}^k[n] &= \max_s \sum_l P\left(y_q^k[n] = s, N_n^k = l \mid \mathbf{z}^k\right). \end{aligned} \tag{15}$$

The symbol-by-symbol MAP estimates are obtained by the application of the BCJR algorithm [26] which, in the case of VLCs, operates on the joint trellis representation of the Markov source and VLC trellis [27, 28]. The MAP estimate can also be obtained by the algorithm which separates the

Markov source model and the VLC model [25]. This approach reduces the complexity of the decoding algorithm.

Due to channel errors, the VLC/FLC decoder occasionally makes an error and outputs a wrong symbol. This can be seen as if the transmitted symbol has been corrupted by the impulse noise of magnitude equal to the difference between the decoded and transmitted symbols.

5. SYNDROME DECODING OF OFB CODES

The signal at the input of the OFB decoder (output of the VLC/FLC decoder) $y_R^k[n]$ can be written as

$$y_R^k[n] = y^k[n] + e^k[n] + n^k[n], \tag{16}$$

where $n^k[n]$ is the quantization noise and $e^k[n]$ is an impulse error at the output of the VLC/FLC decoder in subband k. The quantization noise is modeled as a Gaussian random variable with a zero mean and variance σ_q^2. We consider the two following models for the impulse errors.

5.1. Bernoulli-Gaussian model

The impulse noise is modeled as $e^k[n] = a^k[n]b^k[n]$, where $a^k[n]$ is a sequence of ones and zeros with probability $P(a^k[n] = 1) = p^k$ and $b^k[n]$ is a Gaussian random variable with zero mean and variance $\sigma_I^{k^2}$. The overall noise model is a mixture of the Gaussian and Bernoulli-Gaussian noises [1, 19].

5.2. Quantizer-dependent model

The impulse noise is modeled as $e^k[n] = a^k[n]b^k[n]$, where $a^k[n]$ is a sequence of ones and zeros with probability $P(a^k[n] = 1) = p^k$ and $b^k[n]$ is a discrete random variable with $P(b^k[n] = \Delta_\xi^k) = P_\xi$. In this model, the values Δ_ξ^k are given by the differences between the symbol levels in a subband, while the value $P(b^k[n] = \Delta_\xi^k) = P_\xi^k$ represents the probability that a VLC/FLC decoder outputs a symbol S_ν^k, whereas a symbol $S_\mu^k = S_\nu^k - \Delta_\xi^k$ was transmitted.

The input of the OFB decoder, the corresponding analysis filter bank's outputs, quantization noise, and impulse errors corrupting the analysis filter banks' outputs in various subbands (16) are arranged in an array as

$$\begin{aligned}
\mathbf{y}_R[n] &= \left[y_R^0[n] \ \cdots \ y_R^{N-1}[n]\right]^T,\\
\mathbf{y}[n] &= \left[y^0[n] \ \cdots \ y^{N-1}[n]\right]^T,\\
\mathbf{n}[n] &= \left[n^0[n] \ \cdots \ n^{N-1}[n]\right]^T,\\
\mathbf{e}[n] &= \left[e^0[n] \ \cdots \ e^{N-1}[n]\right]^T, \quad n = 0,\ldots,L-1,
\end{aligned} \tag{17}$$

where $y^k[n] = 0$, $y_R^k[n] = 0$, $n^k[n] = 0$, and $e^k[n] = 0$ for $n < 0$ and $n > L^k - 1$. L^k is the length of the sequences in subband k. In the time domain, the syndrome equations for window j of the received signal can be written as

$$\mathbf{S}^j = \mathbf{P}\mathbf{y}_R^j = \mathbf{P}(\mathbf{y}^j + \mathbf{n}^j + \mathbf{e}^j), \tag{18}$$

where

$$\begin{aligned}
\mathbf{S}^j &= \left[\mathbf{s}^T[j] \ \ \mathbf{s}^T[j+1] \ \cdots \ \mathbf{s}^T[j+M-1]\right]^T,\\
\mathbf{s}[j] &= \left[s_1[j] \ \ s_2[j] \ \cdots \ s_{N-K}[j]\right]^T,\\
\mathbf{y}_R^j &= \left[\mathbf{y}_R^T[j-L_P] \ \cdots \ \mathbf{y}_R^T[j+M-1]\right]^T,\\
\mathbf{y}^j &= \left[\mathbf{y}^T[j-L_P] \ \cdots \ \mathbf{y}^T[j+M-1]\right]^T,\\
\mathbf{n}^j &= \left[\mathbf{n}^T[j-L_P] \ \cdots \ \mathbf{n}^T[j+M-1]\right]^T,\\
\mathbf{e}^j &= \left[\mathbf{e}^T[j-L_P] \ \cdots \ \mathbf{e}^T[j+M-1]\right]^T,
\end{aligned} \tag{19}$$

and $\mathbf{P}$ is a matrix in (11) restricted to dimension $[(N-K)M \times N(M+L_P)]$.

As the number of syndrome equations for an entire OFB encoded sequence is large, the syndrome decoder operates on the segments of the received codeword, in a sequential manner. The decoding algorithm consists of two steps: error localization and error amplitude estimation. The error localization procedure determines the positions in which errors have occurred by inspecting the syndromes. Due to quantization noise, syndromes have nonzero values, even in absence of channel noise. The localization procedure therefore has to distinguish between the changes of syndrome values due to quantization noise and that due to impulse errors. This can be done for example by thresholding the syndrome values [18]. However, better results can be achieved by using more sophisticated methods such as methods based on the hypothesis testing theory [1, 18, 19].

The errors are localized and estimated for the first window of the received signal. Their influence is removed. The decoding procedure for the next syndromeand received data windows $\mathbf{S}^{j+M}$ and $\mathbf{y}_R^{j+M}$ is the same as that for the first window. The typical window size is $M = L_P + 1$.

5.3. Error localization

The approach presented here is based on the M-ary hypothesis testing theory [20], where each possible position of an impulse error within a window of the received data is considered as a separate hypothesis [18]. We further introduce a symbol reliability information provided by a SISO VLC/FLC decoder in this localization procedure.

We assume that impulse errors are sparse and that we can have at most one error within a few consecutive windows of the received data. Each possible position of an impulse error within a window of the received data is considered as a separate hypothesis. The null hypothesis means that there are no impulse errors. We note that in the first window,

$[\mathbf{y}_R^T[-L_P]\cdots\mathbf{y}_R^T[-1]]^T$ is a zero vector. As we assume that there is no error propagation, the first L_PN samples in the following data windows are corrupted only by quantization noise. The effective window size for impulse error localization and correction is therefore MN samples. That is, we consider $MN+1$ hypotheses: null hypothesis H_0 and hypothesis H_i, $i=1,\ldots,MN$ which says that there is an impulse error in position NL_P+i within the window j of the received data $\mathbf{y}_R^j$. This in turn means that there is an error at time instant $n=((j-1)M+\lfloor i/N\rfloor)$ in subband $k=(i \mod N)$. That is, the error position assumed by the hypothesis directly translates into the number of the subband and the time instant in which error has occurred.

5.3.1. Hypothesis testing for a Bernoulli-Gaussian impulse noise model

Assuming that the quantization noise is Gaussian and independent of the impulse noise which has Bernoulli-Gaussian distribution, the joint probability density function (pdf) of the syndromes under hypothesis H_i is a multivariate Gaussian distribution given by

$$p(s_1,\ldots,s_D\mid H_i) = \frac{1}{(2\pi)^{D/2}\det(\mathbf{M}_i)^{1/2}} \times\exp\left(\left[-\frac{1}{2}\left(\mathbf{S}^j-\bar{\mathbf{S}}_i^j\right)^T\mathbf{M}_i^{-1}\left(\mathbf{S}^j-\bar{\mathbf{S}}_i^j\right)\right]\right), \tag{20}$$

where, in order to simplify the notation, the $D=(N-K)M$ elements in $\mathbf{S}^j$ are denoted by $s_1,\ldots s_D$. $\mathbf{M}_i$ is the syndrome covariance matrix under hypothesis H_i, and $\bar{\mathbf{S}}_i^j$ is a vector of syndromes mean values under hypothesis H_i. The quantities $\mathbf{M}_0$ (hypothesis that there is no channel error), $\mathbf{M}_i$, and $\bar{\mathbf{S}}_i^j$ are given by

$$\begin{aligned}\mathbf{M}_0 &= E\left\{\mathbf{S}^j\mathbf{S}^{jT}\mid H_0\right\}\\ &= \mathbf{P}\,\mathrm{diag}\left\{\sigma_q^{0^2},\ldots,\sigma_q^{N-1^2},\ldots,\sigma_q^{0^2},\ldots,\sigma_q^{N-1^2}\right\}\mathbf{P}^T,\\ \mathbf{M}_i &= E\left\{\mathbf{S}^j\mathbf{S}^{jT}\mid H_i\right\}\\ &= \mathbf{P}\left[\mathrm{diag}\left\{\sigma_q^{0^2},\ldots,\sigma_q^{N-1^2},\ldots,\left(\sigma_q^{k^2}+\sigma_I^{k^2}\right),\ldots,\sigma_q^{N-1^2}\right\}\right]\mathbf{P}^T,\\ \bar{\mathbf{S}}_i^j &= E\{\mathbf{S}^j\mid H_i\} = E\{\mathbf{P}\mathbf{y}_R^j\mid H_i\} = \mathbf{0},\end{aligned} \tag{21}$$

where $k=(i \mod N)$.

The a posteriori probability of each hypothesis is given by

$$p(H_i\mid s_1,\ldots,s_D) = \frac{p(s_1,\ldots,s_D\mid H_i)\,p_a(H_i)}{p(s_1,\ldots,s_D)}, \tag{22}$$

where $p_a(H_i)$ is the a priori probability hypothesis H_i, that is, the a priori probability of having an error at position i within the considered window.

5.3.2. Hypothesis testing for a quantizer-dependent impulse noise model

The possible error amplitudes at the output of the VLC/FLC decoder are given by the symbol level differences $\Delta_\xi^k=S_\mu^k-S_\nu^k$, $\mu\neq\nu$, $\mu,\nu=1,\ldots,N_Q^k$, where S_μ^k are symbols in the symbol alphabet of subband k. For example, for a uniform scalar quantization with a dead zone, the quantized symbol values are given by $y_q^k[n]=\mathrm{sign}(I^k[n])|I^k[n]|\delta^k$, where $I^k[n]=\mathrm{sign}(y^k[n])\lfloor|y^k[n]|/\delta^k\rfloor$, and δ^k is the quantization step size in subband k. For this example, the differences between symbol values Δ_ξ^k are given by $\Delta_\xi^k=\pm\nu\delta^k$, $\nu=1,\ldots N_Q^k-1$.

The joint pdf of syndromes conditioned on Δ_ξ^k and H_i is a multivariate Gaussian distribution given by

$$p\left(s_1,\ldots,s_D\mid H_i,\Delta_\xi^k\right) = \frac{1}{(2\pi)^{D/2}\det(\mathbf{M}_i)^{1/2}} \times\exp\left(\left[-\frac{1}{2}\left(\mathbf{S}^j-\bar{\mathbf{S}}_i^j\right)^T\mathbf{M}_i^{-1}\left(\mathbf{S}^j-\bar{\mathbf{S}}_i^j\right)\right]\right), \tag{23}$$

where $\mathbf{M}_i$ and $\bar{\mathbf{S}}_i^j$ are given by

$$\begin{aligned}\mathbf{M}_i &= E\left\{\mathbf{S}^j\mathbf{S}^{jT}\mid H_i\right\}\\ &= \mathbf{P}\,\mathrm{diag}\left\{\sigma_q^{0^2},\ldots,\sigma_q^{N-1^2},\ldots,\sigma_q^{0^2},\ldots,\sigma_q^{N-1^2}\right\}\mathbf{P}^T,\\ \bar{\mathbf{S}}_i^j &= E\{\mathbf{S}^j\mid H_i\} = E\{\mathbf{P}\mathbf{y}_R^j\mid H_i\}\\ &= \mathbf{P}\left[0\ \cdots\ 0\ \ \Delta_\xi^k\ \ 0\ \cdots\ 0\right]^T,\quad \bar{\mathbf{S}}_0^j=\mathbf{0},\end{aligned} \tag{24}$$

where $k=(i \mod N)$.

In this case, the hypothesis is characterized by the parameter Δ_ξ^k which can take a number of different values. Assuming that we know the probability distribution $P(\Delta_\xi^k\mid H_i)$, we can apply the composite hypothesis testing. The a posteriori probability of the hypothesis is given by

$$p(H_i\mid s_1,\ldots,s_D) = \frac{\sum_{\Delta_\xi^k}p(s_1,\ldots,s_D\mid H_i,\Delta_\xi^k)P(\Delta_\xi^k\mid H_i)\,p_a(H_i)}{p(s_1,\ldots,s_D)}, \tag{25}$$

where $P(\Delta_\xi^k=0\mid H_0)=1$ and where we have assumed that the probability of making an error Δ_ξ^k does not depend on the error position, that is, $P(\Delta_\xi^k\mid H_i)=P(\Delta_\xi^k)=P_\xi^k$.

5.4. The hypothesis a priori probabilities

The a priori probability of each hypothesis can be calculated based on the average symbol error rate (SER) at the output

of the VLC/FLC decoder or based on the symbol posteriori marginals provided by the SISO VLC/FLC decoder.

5.4.1. Using the average SER

The a priori probabilities are given by

$$\begin{aligned} p_a(H_0) &= (1-p^k)^{MN}, \\ p_a(H_i) &\approx (1-p^k)^{MN-1}p^k, \quad i = 1,\ldots,MN, \end{aligned} \tag{26}$$

where p^k is the probability of an impulse error in the subband k.

5.4.2. Using the symbol posteriori marginals

The a priori probabilities are given by

$$\begin{aligned} p_a(H_0) &= \prod_{v} P[v], \\ p_a(H_i) &= (1-P[i])\prod_{v\neq i} P[v], \quad i = 1,\ldots,MN, \end{aligned} \tag{27}$$

where $P[v]$ is an element of a vector of symbol probabilities $\mathbf{P} = [P[0]\cdots P[MN-1]]$ obtained by interlacing the probabilities at the output of the SISO VLC/FLC decoders in various subbands as

$$\mathbf{P} = \left[P^0[j] \;\cdots\; P^{N-1}[j] \;\cdots\; P^0[j+M-1] \;\cdots\; P^{N-1}[j+M-1]\right]. \tag{28}$$

The OFB decoding algorithm with calculation of the a priori probabilities as in (26) and (27) is referred to as Algorithms A and B, respectively.

5.5. Error tracking

Due to the memory of the convolutional code, the errors can be tracked by considering syndrome segments $\mathbf{S}^{j+1}\cdots\mathbf{S}^{j+L_P}$ under the same set of hypothesis as in the window corresponding to $\mathbf{S}^j$ [18]. That is, the hypothesis testing should indicate the same error location in respect to window $\mathbf{S}^j$ for each of these syndrome segments. We therefore introduce a parameter T which specifies how many times the error location has to be confirmed in order to be considered as a true error location. The tracking of errors is necessary if the structure of the matrix $\mathbf{P}$ in (11) is such that not all error positions can be detected by considering only the syndrome segment $\mathbf{S}^j$.

5.6. Amplitude estimation

Once located, the errors' amplitudes are calculated by solving the syndrome equations in (18) in the least-square sense. For the error at position i within a window $\mathbf{y}_R^j$, the error amplitude is estimated as

$$e_i^j = \left(\mathbf{P}_i^T\mathbf{P}_i\right)^{-1}\mathbf{P}_i^T\mathbf{S}^j. \tag{29}$$

$\mathbf{P}_i$ denotes the ith column of matrix $\mathbf{P}$. Since impulse errors are sparse, one can consider additional syndrome equations in order to have better estimate of the error amplitudes. It is necessary to consider additional syndrome equations when the matrix $\mathbf{P}$ in (11) is such that the system of syndrome equations in (7) is underdetermined for some error positions. For the amplitude estimation, we consider a set of equations corresponding to the following augmented syndrome segment $[\mathbf{S}^{j\,T}\;\; \mathbf{s}^T[j+M] \;\cdots\; \mathbf{s}^T[j+M+E-1]]^T$, where E is a parameter which determines the number of additional syndrome equations. After amplitude estimation, the error estimates for particular subband and time instant are subtracted from the received signal.

5.7. Message reconstruction

It has been shown in [14] that if the output of an OFB is corrupted by quantization error which can be modeled by an additive white noise, and if the noise sequences in different channels are pairwise uncorrelated, the pseudoinverse is the best linear reconstruction operator in the mean-square sense. Assuming that after impulse error correction the received sequence is corrupted only by quantization noise, the message is reconstructed by applying the pseudoinverse receiver.

The polyphase matrix of the synthesis filter bank corresponding to the pseudoinverse receiver is obtained as

$$\mathbf{R}(z) = \left[\widetilde{\mathbf{E}}(z)\mathbf{E}(z)\right]^{-1}\widetilde{\mathbf{E}}(z), \tag{30}$$

where $\widetilde{\mathbf{E}}(z) = \mathbf{E}^H(1/z^*)$ denotes the paraconjugate of $\mathbf{E}(z)$.

6. ITERATIVE DECODING OF THE OFB-FLC CHAIN

Here we consider joint decoding of an OFB-FLC code and present an iterative algorithm which can improve the decoding performance. However, we do not give the proof for the convergence of this algorithm.

The syndrome decoding algorithm computes the a posteriori probabilities of the hypothesis regarding the impulse error positions. As the symbols at the input of the OFB syndrome decoder are known, the calculated a posteriori probabilities can be used to "eliminate" particular symbols from the trellis in the SISO FLC decoding algorithm in the next iteration. For example, if the a posteriori probability of hypothesis H_i is 1, this means that the decoded symbol at time instant corresponding to the error position assumed by hypothesis H_i is wrong. This symbol can therefore be eliminated from the trellis of the Markov source. The SISO decoding can thus be performed on the reduced trellis. That is, in this way, the trellis for SISO decoding can be iteratively

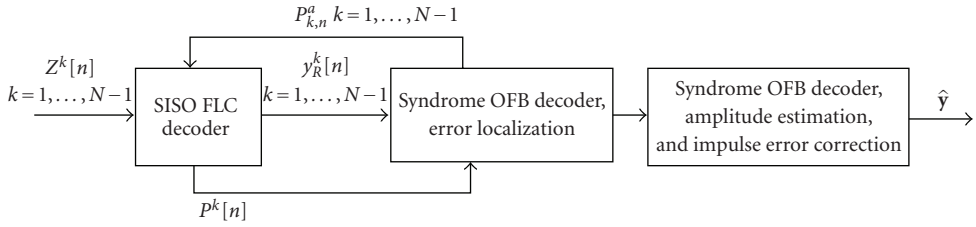

Figure 3: Block diagram of the iterative decoder.

pruned. The block diagram of the iterative decoder is shown in Figure 3.

The pruning of the trellis in the FLC decoder is done by multiplying the $\alpha_n(s)$ and $\beta_n(s)$ coefficients in (14) by a factor $P^a_{k,n}(s)$ in the following way: $\alpha_n(s) = \sum_{s'} \alpha_{n-1}(s')\gamma_n(s', s)P^a_{k,n}(s)$ and $\beta_n(s) = \sum_{s'} \beta_{n+1}(s')\gamma_{n+1}(s, s')P^a_{k,n+1}n(s')$. The probability $P^a_{k,n}(s)$ is the a priori probability of the state s at time instant n in the trellis for subband k. The probabilities $P^a_{k,n}(s)$ are initialized to 1 in the first iteration. In the subsequent iterations,the probabilities $P^a_{k,n}(s)$ are updated for the decoded symbols for which an error has been detected in the OFB syndrome decoder in the previous iteration. That is, let us assume that in iteration $r-1$, the errors have been detected for the subset of decoded symbols given by $[\hat{y}^k_q[n_0] = s_{n_0}\ \hat{y}^k_q[n_1] = s_{n_1}\ \cdots\ \hat{y}^k_q[n_t] = s_{n_t}]$, $s_{n_m} \in \mathcal{S}^k$. The probabilities $P^a_{k,n}(s)$ in iteration r, denoted in the following by $P^a_{k,n,r}(s)$, are updated as

$$P^a_{k,n,r}(s_n) = P^a_{k,n,r-1}(s_n)\left(1 - P^{\text{app}}_{k,n,r-1}(s_n)\right), \quad n = n_0, \ldots, n_t, \tag{31}$$

where $P^{\text{app}}_{k,n,r}(s_n)$ is the a posteriori probability of the hypothesis H_i which, since there is a one-to-one correspondence between the error position in the window of received data and the subband and time indices, says that there is an error at time instant n and subband k. Knowing that the OFB syndrome decoder input in iteration r was $y_R[n] = s_n$, the $P^{\text{app}}_{k,n,r}(s_n)$ can be seen as the probability that the symbol s_n was not transmitted at time instant n in subband k.

There are two problems associated with this iterative algorithm. First, the a posteriori probabilities of the hypothesis are calculated for a number of consecutive overlapping windows of syndromes and the question which one to use as $P^{\text{app}}_{k,n,r}(s_n)$. Here, we take an empirical approach and use the average of the hypothesis a posteriori probabilities over the considered syndrome windows. The second problem is the presence of the false detected errors. Due to false detected errors, it is possible that the performance of the algorithm decreases with iterations. However, assuming that the probability of a false alarm is small and that in the case of false detected errors the probabilities $P^{\text{app}}_{k,n,r}(s_n)$ are small, we can expect the MSE improvement with iterations. Also, in most cases if a false detected error in one iteration becomes a true error in the next iteration due to soft "elimination" of the correct state, it will be detected by the syndrome decoder and corrected. The experimental results show that the MSE decreases with iterations and stabilizes after a few iterations around a value smaller than the MSE obtained in the first iteration.

7. PERFORMANCE RESULTS

In this section, we consider an application of the presented decoding algorithm to an image coding system with a tree-structured subband signal decomposition shown in Figure 4. In each stage, an $N = 2$-channel biorthogonal 9/7 wavelet filter bank is employed.

The redundant signal representation is obtained by removing the downsamplers in the last horizontal filtering stage. Therefore, the signal in the first two subbands is protected by the OFB code with $(N, K) = (2, 1)$. The generator and parity check matrices of an OFB are given by $\mathbf{E}(z) = [H_0(z)\ \ H_1(z)]^T$ and $\mathbf{P}(z) = [H_1(z)\ \ -H_0(z)]$, where $H_0(z)$ and $H_1(z)$ are the z transforms of the two-channel wavelet filter bank impulse responses.

We assume that the oversampling is introduced in the last horizontal filtering stage, whereas VLC/FLC coding is applied on the columns of the 2D subband representation of an image. The JSC codeword is depicted in Figure 5. In the case of the system with a VLC, this kind of interleaving prevents bursty impulse errors at the output of the entropy decoder. The interleaving also facilitates iterative decoding of the OFB-FLC chain.

All the results are obtained for the gray scale $[512 \times 512]$ Lena image. The Markov model parameters are estimated by simulation. The parameters E and T are set to $E = 5$ and $T = 5$. The number of quantization levels in subbands LL2, LH2, HL2, HH2, LH1, HL1, and HH1 is 64, 16, 4, 4, 2, 2, and 2, respectively.

Tables 1 and 2 show the performance of various decoding algorithms in terms of the mean-square error (MSE), the probability of detection P_d, and the probability of a false alarm P_f. The probability of detection is the probability that we localize an error when there is an error. The probability of a false alarm is the probability that we localize an error when in fact there is no impulse error at that position. The results compare the performance of the syndrome decoding Algorithms A and B with Bernoulli-Gaussian impulse noise model. The results for the quantizer-dependent impulse noise model are not shown as they are similar to the results for the Bernoulli-Gaussian impulse noise model. The decoding algorithm with no syndrome decoding is referred to as pseudoinverse receiver (PR). Table 1 shows the results in the system with a Huffman entropy code. The MSE

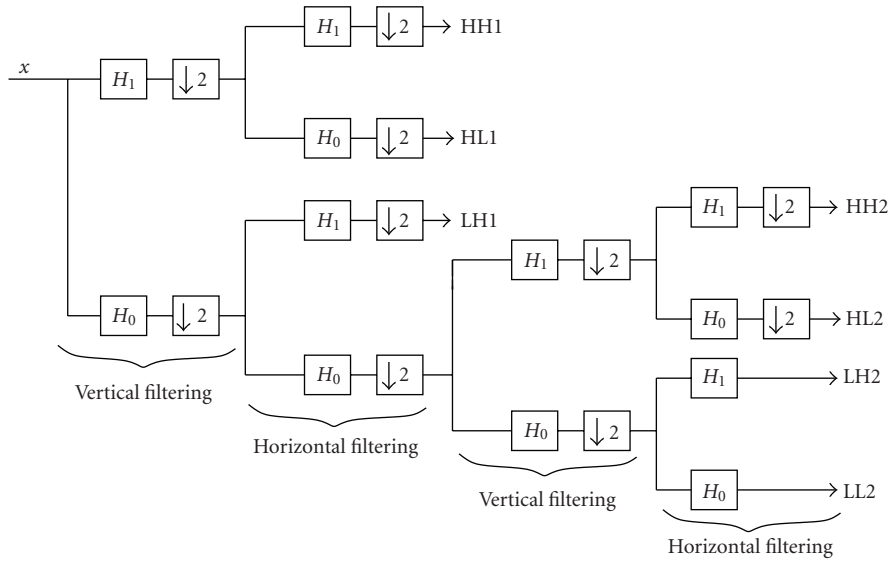

Figure 4: Structure of an OFB.

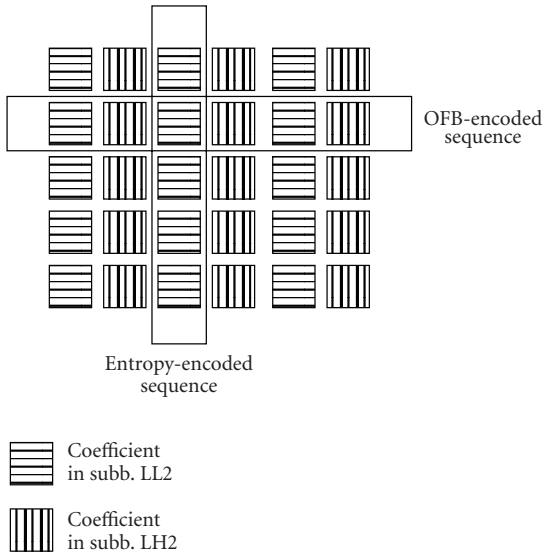

Figure 5: JSC codeword.

in the absence of channel noise is 43.3804. The probabilities of impulse errors at the output of a VLC decoder in the first two subbands are $p_{LL2} = 0.0053$ and $p_{LH2} = 0.0077$ for $E_b/N_0 = 5$ dB, and $p_{LL2} = 0.0116$ and $p_{LH2} = 0.0182$ for $E_b/N_0 = 4$ dB. The impulse-to-quantization noise ratio in the first two subbands are $\text{IQR}_{LL2} = 23.54$ dB and $\text{IQR}_{LH2} = 16.4$ dB for $E_b/N_0 = 5$ dB, and $\text{IQR}_{LL2} = 24.12$ dB and $\text{IQR}_{LH2} = 16.6$ dB for $E_b/N_0 = 4$ dB.

Table 2 shows the results in the system with an FLC. The MSE in the absence of channel noise is 21.8339. The probabilities of impulse errors at the output of FLC decoders in the first two subbands are $p_{LL2} = 0.0055$ and $p_{LH2} = 0.0067$ for $E_b/N_0 = 6$ dB, and $p_{LL2} = 0.0282$ and $p_{LH2} = 0.0344$ for $E_b/N_0 = 4$ dB. The impulse-to-quantization noise ratios are $\text{IQR}_{LL2} = 24.9965$ dB and $\text{IQR}_{LH2} = 14.8449$ dB for $E_b/N_0 = 6$ dB, and $\text{IQR}_{LL2} = 25.5188$ dB and $IRQ_{LH2} = 14.7$ dB for $E_b/N_0 = 4$ dB. We assume natural binary index assignment.

From Tables 1 and 2, we can see that introducing the soft information in the localization procedure of the syndrome decoding algorithm significantly improves the probability of a detection. In the system with an FLC code, the probability of a false alarm is decreased as well. In the system with a VLC code, the probability of a false alarm is decreased in the subband LL2 where the IQR is high. However, in the LH2 subband where the IQR is low, utilizing the soft information can worsen the probability of a false alarm. In both systems, the MSE performance of Algorithms A and B is similar.

The peak signal-to-noise (PSNR) improvement due to OFB syndrome decoding at $E_b/N_0 = 4$ dB is 0.75 dB for the system with an FLC and 0.6 dB for the system with a VLC. We have assumed that the entropy decoders perfectly know the Markov model parameters. In this case, the SISO entropy decoding performs very well, that is, the IQR is small. The possible improvement by using a syndrome decoding algorithm is therefore small. For example, in the system with the FLC, the maximum possible PSNR gain due to syndrome decoding is less than 1.18 dB at $E_b/N_0 = 4$ dB and less than 0.24 dB at $E_b/N_0 = 6$ dB. As the other extreme, we consider a system with the FLC and entropy decoding which does not make use of the Markov property of the source symbols in the first two subbands. For this example, the MSE for $E_b/N_0 = 6$ dB in the system with and without syndrome decoding is 22.87847 and 40.411473.

Figures 6 and 7 show the reconstructed image without and with syndrome decoding for this example.

Figure 8 shows the MSE versus E_b/N_o for the first and the fourth iterations in the iterative decoding of the OFB-FLC chain. The results for the pseudoinverse receiver and the performance of the pseudoinverse receiver in the case when there are no impulse errors in the first two subbands are also

Table 1: Performance of the syndrome decoding algorithm in the system with a VLC.

MSE	P_d^{LL2}	P_d^{LH2}	P_f^{LL2}	P_f^{LH2}	Alg.	E_b/N_0
44.6844	0.4298	0.4006	0.0004	0.0006	A	5 dB
44.4559	0.5516	0.5370	0.0002	0.0013	B	5 dB
48.2196	—	—	—	—	PR	5 dB
48.7849	0.3978	0.3218	0.0011	0.0014	A	4 dB
48.1248	0.4851	0.4046	0.0007	0.0027	B	4 dB
55.3454	—	—	—	—	PR	4 dB

Table 2: Performance of the syndrome decoding algorithm in the system with an FLC.

MSE	P_d^{LL2}	P_d^{LH2}	P_f^{LL2}	P_f^{LH2}	Alg.	E_b/N_0
21.9933	0.4981	0.2349	0.0006	0.0055	A	6 dB
21.9697	0.6418	0.3399	0.0005	0.0031	B	6 dB
23.0284	—	—	—	—	PR	6 dB
24.2307	0.4231	0.1981	0.0015	0.0051	A	4 dB
24.0243	0.5124	0.2533	0.0010	0.0037	B	4 dB
28.7464	—	—	—	—	PR	4 dB

Figure 6: Reconstructed image, no syndrome decoding.

Figure 7: Reconstructed image after syndrome decoding.

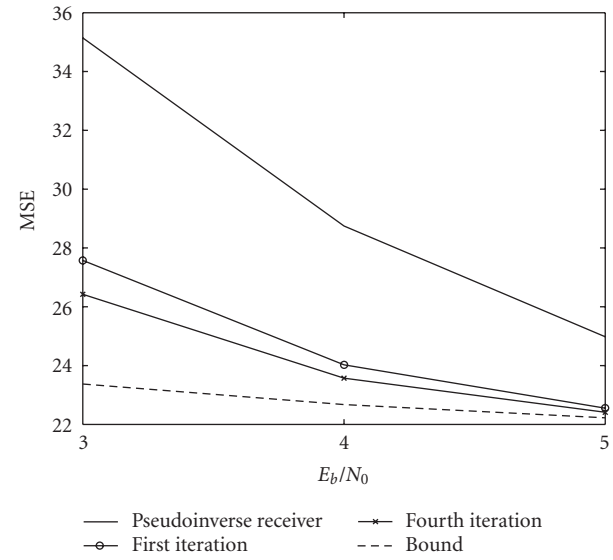

Figure 8: Performance of the iterative decoding of the OFB-FLC chain.

shown. From this figure, we can see that iterative decoding reduces the MSE. However, at 3 dB, there is still a significant gap between the performance in the fourth iteration and the performance of the system with no impulse errors in the first two subbands.

8. CONCLUSIONS

We have examined the performance of a JSCC system consisting of OFB codes and of redundant source codes. The localization procedure based on the M-ary hypothesis testing theory for the two impulse noise models has been developed. We have further shown how the soft information at the output of the SISO entropy decoder can be used in order to

improve the error localization procedure. An empirical algorithm for the iterative decoding of the FLC-OFB chain has been presented. The performance of the various decoding algorithms has been tested for the image compression system with a wavelet-based signal decomposition.

ACKNOWLEDGMENT

A part of this work has been presented in the EUSIPCO '04 and GLOBECOM '04 conferences.

REFERENCES

[1] G. R. Redinbo, "Decoding real block codes: activity detection Wiener estimation," *IEEE Transactions on Information Theory*, vol. 46, no. 2, pp. 609–623, 2000.

[2] J. Wolf, "Redundancy, the discrete Fourier transform, and impulse noise cancellation," *IEEE Transactions on Communications*, vol. 31, no. 3, pp. 458–461, 1983.

[3] J.-L. Wu and J. Shiu, "Discrete cosine transform in error control coding," *IEEE Transactions on Communications*, vol. 43, no. 5, pp. 1857–1861, 1995.

[4] V. K. Goyal, J. Kovacevic, and M. Vetterli, "Quantized frame expansions as source-channel codes for erasure channels," in *Proceedings of Data Compression Conference (DCC '99)*, pp. 326–335, Snowbird, Utah, USA, March 1999.

[5] G. Rath and C. Guillemot, "Performance analysis and recursive syndrome decoding of DFT codes for bursty erasure recovery," *IEEE Transactions on Signal Processing*, vol. 51, no. 5, pp. 1335–1350, 2003.

[6] G. Rath and C. Guillemot, "Frame-theoretic analysis of DFT codes with erasures," *IEEE Transactions on Signal Processing*, vol. 52, no. 2, pp. 447–460, 2004.

[7] F. Marvasti, M. Hasan, M. Echhart, and S. Talebi, "Efficient algorithms for burst error recovery using FFT and other transform kernels," *IEEE Transactions on Signal Processing*, vol. 47, no. 4, pp. 1065–1075, 1999.

[8] T. G. Marshall Jr., "Coding of real-number sequences for error correction: a digital signal processing problem," *IEEE Journal on Selected Areas in Communications*, vol. 2, no. 2, pp. 381–392, 1984.

[9] R. E. Blahut, *Algebraic Methods for Signal Processing and Communications Coding*, Springer, New York, NY, USA, 1992.

[10] S. Mehrotra and P. A. Chou, "On optimal frame expansions for multiple description quantization," in *Proceedings of IEEE International Symposium on Information Theory (ISIT '00)*, pp. 176–176, Sorrento, Italy, June 2000.

[11] G. Rath and C. Guillemot, "Characterization of a class of error correcting frames and their application to image transmission," in *Proceedings of Picture Coding Symposium*, Saint-Malo, France, April 2003.

[12] G. Rath and C. Guillemot, "Subspace algorithms for error localization with DFT codes," in *Proceedings of IEEE International Conference on Acoustics, Speech, and Signal Processing (ICASSP '03)*, vol. 4, pp. 257–260, Hong Kong, China, April 2003.

[13] A. Gabay, O. Rioul, and P. Duhamel, "Joint source-channel coding using structured oversampled filters banks applied to image transmission," in *Proceedings of IEEE International Conference on Acoustics, Speech, and Signal Processing (ICASSP '01)*, vol. 4, pp. 2581–2584, Salt Lake City, Utah, USA, May 2001.

[14] J. Kovacevic, P. L. Dragotti, and V. K. Goyal, "Filter bank frame expansions with erasures," *IEEE Transactions on Information Theory*, vol. 48, no. 6, pp. 1439–1450, 2002.

[15] P. L. Dragotti, S. D. Servetto, and M. Vetterli, "Optimal filter banks for multiple description coding: analysis and synthesis," *IEEE Transactions on Information Theory*, vol. 48, no. 7, pp. 2036–2052, 2002.

[16] P. L. Dragotti, J. Kovacevic, and V. K. Goyal, "Quantized oversampled filter banks with erasures," in *Proceedings of Data Compression Conference (DCC '01)*, pp. 173–182, Snowbird, Utah, USA, March 2001.

[17] R. Motwani and C. Guillemot, "Tree-structured oversampled filter banks as joint source-channel codes: application to image transmission over erasure channels," *IEEE Transactions on Signal Processing*, vol. 52, no. 9, pp. 2584–2599, 2004.

[18] G. R. Redinbo, "Decoding real-number convolutional codes: change detection, Kalman estimation," *IEEE Transactions on Information Theory*, vol. 43, no. 6, pp. 1864–1876, 1997.

[19] J. C. Chiang, M. Kieffer, and P. Duhamel, "Oversampled filter banks seen as channel codes: impulse noise correction," in *Proceedings of IEEE International Conference on Acoustics, Speech, and Signal Processing (ICASSP '03)*, vol. 4, pp. 249–252, Hong Kong, April 2003.

[20] H. L. Van Trees, *Detection, Estimation, and Modulation Theory*, John Wiley & Sons, New York, NY, USA, 1968.

[21] H. Bölcskei and F. Hlawatsch, "Oversampled filter banks: optimal noise shaping, design freedom, and noise analysis," in *Proceedings of IEEE International Conference on Acoustics, Speech, and Signal Processing (ICASSP '97)*, vol. 3, pp. 2453–2456, Munich, Germany, April 1997.

[22] S. Weiss, "On the design of oversampled filter banks for channel coding," in *Proceedings of 12th European Signal Processing Conference*, pp. 885–888, Vienna, Austria, September 2004.

[23] Z. Cvetkovic and M. Vetterli, "Oversampled filter banks," *IEEE Transactions on Signal Processing*, vol. 46, no. 5, pp. 1245–1255, 1998.

[24] P. P. Vaidyanathan, *Multirate Systems and Filter Banks*, Prentice-Hall, Englewood Cliffs, NJ, USA, 1993.

[25] A. Guyader, E. Fabre, C. Guillemot, and M. Robert, "Joint source-channel turbo decoding of entropy-coded sources," *IEEE Journal on Selected Areas in Communications*, vol. 19, no. 9, pp. 1680–1696, 2001.

[26] L. Bahl, J. Cocke, F. Jelinek, and J. Raviv, "Optimal decoding of linear codes for minimizing symbol error rate," *IEEE Transactions on Information Theory*, vol. 20, no. 2, pp. 284–287, 1974.

[27] R. Bauer and J. Hagenauer, "Iterative source/channel decoding based on a trellis representation for variable length codes," in *Proceedings of IEEE International Symposium on Information Theory (ISIT '00)*, pp. 238–238, Sorrento, Italy, June 2000.

[28] C. Weidmann and P. Siohan, "Décodage conjoint source-canal avec estimation en ligne de la sourc," in *Proceedings of COmpression et REprésentation des Signaux Audiovisuels (CORESA '03)*, pp. 105–108, Lyon, France, January 2003.

Slavica Marinkovic received her B.S. degree in electrical engineering from The University of Belgrade, Serbia and Montenegro, in 1997, and a Ph.D. degree from The University of Sydney, Australia, in 2002. Since 2002, she has been working with IRISA-INRIA, Rennes, France. Her research interests are in CDMA, error-control coding, and joint source-channel coding.

Christine Guillemot is currently 'Directeur de Recherche' at INRIA, in charge of a research group dealing with image modeling, processing, and video communication. She holds a Ph.D. degree from ENST (École Nationale Supérieure des Télécommunications), Paris. From 1985 to October 1997, she has been with France Télécom/CNET, where she has been involved in various projects in the domain of coding for TV, HDTV, and multimedia applications. From January 1990 to mid-1991, she has worked at Bellcore, NJ, USA, as a Visiting Scientist. Her research interests are signal and image processing, video coding, and joint source-channel coding for video transmission over the Internet and over wireless networks. She has served (2000–2003) as an Associate Editor for IEEE Transactions on Image Processing and is currently an Associate Editor for IEEE Transactions on Circuits and Systems for video technology.